Lasers in Manufacturing Conference 2021

Studies on the direction-independent temperature measurement of a coaxial laser metal deposition process with wire

Avelino Zapata[a,*], Christian Bernauer[a], Melanie Hell[a], Michael F. Zaeh[a]

[a]*Institute for Machine Tools and Industrial Management, Technical University of Munich, Boltzmannstr. 15, 85748 Garching, Germany*

Abstract

Among the Directed Energy Deposition (DED) processes, Laser Metal Deposition with wire (LMD-w) combines the advantages of a high precision and a high deposition rate. Recently, optical systems have been developed that form a ring-shaped laser spot, facilitating a direction-independent LMD-w process. When a pyrometer is coupled to such an optical system, the measurement spot features a ring-shaped form corresponding to the laser spot. Using this pyrometer setup, the inline temperature signal during the LMD-w process was studied within this work. The two modalities of a one-color and a two-color measurement were compared regarding their reliability. The measurement setup was varied to study the influence of different process conditions on the signal. Based on this, a configuration was identified that allowed a valid measurement. A reliable inline temperature measurement opens the opportunity to monitor and control the process.

Keywords: Laser Metal Deposition; DED; Additive Manufacturing; temperature monitoring; one-color pyrometry; two-color pyrometry

1. Introduction

1.1. Motivation

Directed Energy Deposition (DED) processes become increasingly important for Additive Manufacturing (AM) since they allow the production of large freeform parts at high material deposition rates (DebRoy et

* Corresponding author. Tel.: +49 89 289 15572; fax: +49 89 289 15444.
E-mail address: avelino.zapata@iwb.tum.de.

al., 2018). These processes involve the controlled melting of material fed to the process area as wire or powder. The melting can be induced by an electric arc, a laser beam, or an electron beam. The laser-based processes, also called Laser Metal Deposition (LMD) processes, allow a focused and precise energy input and, in contrast to the processes using an electron beam, do not require a vacuum chamber. Therefore, LMD is a preferable AM technology used in the industry to manufacture near-net-shape parts (Dass and Moridi, 2019). When a wire is used, it is often fed laterally to the process, resulting in a leading or trailing configuration, depending on the movement direction. A coaxial alignment of the laser beam and the wire is more advantageous since it allows a direction-independent process in which the wire and the laser beam are perpendicular to the substrate (Kelbassa et al., 2019). This coaxial alignment can be achieved by means of optical elements that form a laser beam with a ring-shaped profile (Kuznetsov et al., 2016; Liu et al., 2014).

The process temperature is crucial for all DED processes as it affects the geometrical and mechanical properties of the produced parts. It is, therefore, of particular interest for in-situ process monitoring and control (Everton et al., 2016). Contactless temperature measurement methods such as pyrometry are used for these applications since they can be flexibly integrated into production systems. For temperature measurements during LMD, the pyrometer usually is aligned laterally to the laser head. It was shown that the geometry of the produced part and the degree of surface oxidation influence the temperature measurement (Bi et al., 2013). Parameter studies were conducted to correlate the process temperature to the laser power, the shielding gas flow, and the laser spot size (Hua et al., 2008). Another study showed that by using two pyrometers, the temperature at the center and the rear part of the melt pool could be measured, allowing to determine a cooling rate (Nair et al., 2020).

In the coaxial LMD process with wire, the wire is fed to the center of the melt pool. Hence, for the described lateral alignment of the pyrometer, the measurement spot of the pyrometer, or short: pyrometer spot, needs to be positioned on an area next to the wire. This area is located in the front, the side, or the rear part of the melt pool, depending on the movement direction of the process. Since different temperatures are present in these areas of the melt pool, a direction-independent temperature measurement is challenging. A solution to this challenge is the direct coupling of the pyrometer into the optical system so that the resulting pyrometer spot has the same ring-shape as the laser spot. This allows equal measurement conditions for any lateral movement direction. However, studies are needed that help to better understand the influence of the ring-shape and the increased size of the pyrometer spot as well as the wire on the temperature signal. Therefore, the temperature signal resulting from different measurement setups was analyzed in this work. At first, a practical method for the calibration of the pyrometer was implemented. Then, three different sizes of the measurement spot were investigated for the temperature measurement of processes with and without wire feed. Finally, based on the resulting temperature signals, the influence of the pyrometer spot size and the wire was evaluated.

1.2. Fundamentals

Plank's law precisely describes the radiance of a surface depending on the temperature and the wavelength. However, because of its simplicity, Wien's approximation to Plank's law is commonly used to formulate this dependency for technical purposes. The spectral radiance L_λ calculated with Wien's approximation differs from the one calculated with Plank's law by less than 1 % if $\lambda \cdot T < 3125$ µm K, which can be assumed to be fulfilled for the following investigations, with λ being the wavelength and T being the temperature (Müller and Renz, 2001). For a black body, Wien's approximation can be written as

$$L_\lambda = \frac{c_1}{\lambda^5} \cdot \frac{1}{e^{\frac{c_2}{\lambda \cdot T}}} \tag{1}$$

with the radiation constants c_1 = 3.742·10^{-16} W m^2 and c_2 = 1.439·10^{-2} m K (Mohr et al., 2012). This formula is crucial for pyrometry measurements as it is used to calculate the temperature based on a measured radiance at a chosen wavelength. Since the black body represents an ideal object, the ratio between the radiance from a real body and a black body, described by the emissivity ε, is needed for the calculation. Therefore, the knowledge of the emissivity of the body at a specified wavelength is essential for one-color measurements. In contrast, for two-color measurements, the radiance is measured at two different wavelengths λ_1 and λ_2, and an emissivity ratio $\varepsilon_1/\varepsilon_2$ is used to calculate the temperature. Under certain conditions, some advantages arise when using the emissivity ratio for temperature measurements. First, if the condition $\varepsilon_1 \approx \varepsilon_2$ is satisfied, the calculated temperature is independent of the emissivity of the body. Second, if $\varepsilon_1/\varepsilon_2$ is constant for the temperature range of interest, the temperature measurement is not influenced by process disturbances that affect the radiance at both wavelengths, e.g., shielding effects from metal vapor or spatters. Third, the temperature of objects smaller than the pyrometer spot can be measured because the temperature value obtained with this method approximately corresponds to the highest temperature within the measurement area (Mates et al., 2002).

2. Experimental

2.1. Materials

AISI 304 substrate plates with a width and length of 100 mm and a thickness of 10 mm and an AISI 308L wire with a diameter of 1 mm were used in the experiments. The chemical composition of both materials is shown in table 1.

Table 1. Chemical composition of the substrate (AISI 304) and the wire (AISI 308L) by mass percentage

Material	C in %	Si in %	Mn in %	P in %	S in %	Cr in %	Ni in %
AISI 304	≤ 0.07	≤ 1.00	≤ 2.00	≤ 0.05	≤ 0.02	17.50–19.50	8.00–10.50
AISI 308L	≥ 0.03	0.65–1.20	1.00–2.50	≤ 0.03	≤ 0.02	19.00–21.00	9.00–11.00

2.2. Systems

The coaxial deposition head *CoaxPrinter* (Precitec GmbH & Co. KG, Germany) reshaped the laser beam by means of a combination of axicons to obtain a hollow laser beam resulting in a ring-shaped beam profile. The laser beam source was an 8 kW multi-mode fiber laser *YLR-8000* (IPG Laser GmbH, Germany) emitting at a wavelength of 1070 nm. For temperature measurements, a two-color pyrometer, also called quotient pyrometer, *METIS M322* (Sensortherm GmbH, Germany) with a temperature measurement range between 600 and 2300 °C and a response time of 1 ms was utilized. The spectral ranges of the first and the second channel (*C1* and *C2*) were 1.65–1.80 µm and 1.45–1.65 µm, respectively. This pyrometer allowed simultaneous one-color and two-color measurements. The temperature source *HE1200* (Sensortherm GmbH, Germany) with an adjustable temperature between 100 °C and 1100 °C was used for the calibration.

2.3. Methods

To compensate for radiance losses within the optical system that negatively influence the measurement, a single-point calibration was conducted based on a constant temperature provided by the temperature source. The calibration temperature of 1080 °C was measured by means of a thermocouple placed on the heating unit

of the temperature source. To determine the emissivity of the molten material, a method implemented by Furumoto et al., 2013 was adapted. This method is based on melting the surface of the material with the least possible energy input so that the melting temperature is just reached or only narrowly exceeded. To keep process-induced melt pool dynamics low, a small melt pool is advantageous. In a small melt pool, a homogeneous temperature distribution can be assumed and steadier surface conditions (e.g., less fluctuation of the liquid surface, which would lead to different angles of radiation) of the melt pool can be expected. Therefore, the laser beam and the pyrometer spot were concentrically aligned and focused on the surface of the substrate, resulting in a solid circular laser spot. Singe tracks with a length of 80 mm were produced, where only the laser beam source was engaged. Since no additional wire was fed, there was no material applied to the surface. The laser power P was increased by 50 W for every track, from 50 W to 250 W, and the traverse speed was set to 3 m/min. The surface of the substrate was then analyzed with a profilometer to examine at which laser power the first signs of melting could be identified. It was assumed that the temperature within the area of the pyrometer spot was approximately equal to the melting temperature for the tracks where the first continuous melting occurred. The emissivities used for the one-color measurements and the emissivity ratio used for the two-color measurement were then adjusted so that the indicated temperature was equal to the melting temperature. Based on the melting ranges of both the substrate and the wire material, a melting temperature of 1450 °C was chosen.

For further experiments, the working distance of the laser head was changed to achieve a ring-shaped laser spot on the surface of the substrate that allowed the coaxial wire feed. The distance between the surface of the substrate and the focal plane of the laser (which was below the surface of the substrate) is described by the focal offset, which determines the size of the ring-shaped laser spot. A 6 mm focal offset was chosen, resulting in a ring-shaped laser spot with an inside diameter of 1.2 mm and an outside diameter of 1.8 mm. This focal offset yielded a stable process. By means of an individual focus unit, it was possible to adjust the size of the pyrometer spot without altering the size of the laser spot. To measure the dimensions of the pyrometer spot, an iris diaphragm was used. The pyrometer was pointed onto the temperature source and the iris diaphragm was placed in between with a fully opened aperture. By gradually reducing the size of the aperture, the diaphragm progressively intersected the radiance detected by the pyrometer. The reduction of the measured radiance lowered the perceived temperature and, thus, allowed to determine the boundaries of the pyrometer spot. Because the temperature change occurred gradually, a threshold of 95 % of the initial temperature was chosen to define the boundaries.

Three pyrometer spot sizes (denoted as small, medium-sized, and large) were set for the temperature measurement. The sizes of the corresponding inner diameters d_i and the outer diameters d_o are illustrated in figure 1. In the experiments, the temperatures T_{C1} and T_{C2} resulting from the one-color measurements and the temperature T_Q resulting from the two-color measurement were observed. The experiments were conducted with a laser power of 1600 W and a traverse speed of 1 m/min. The width of the resulting tracks was

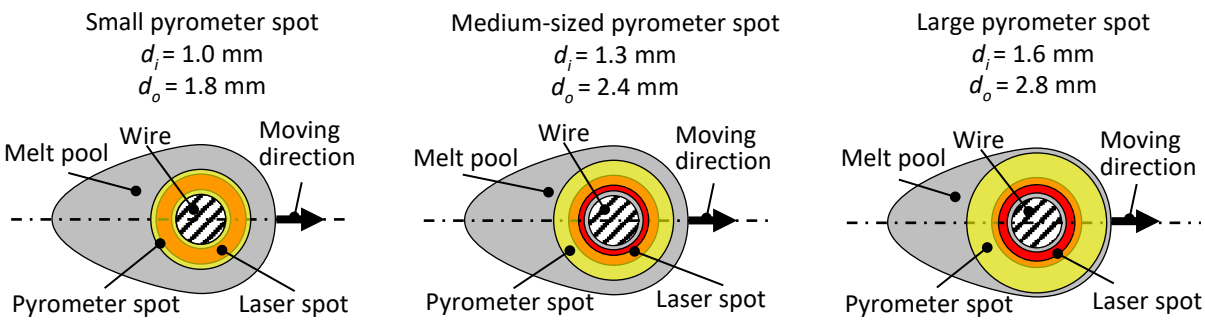

Fig. 1. Schematic illustrations of the measurement setups for small, medium-sized, and large pyrometer spots

3 mm. To analyze the influence of the additional wire feed on the temperature measurement, the experiments were first conducted without wire feed and then with a wire speed of 1 m/min.

3. Results

3.1. Emissivity calibration

The three height profiles of the surfaces of the tracks produced with laser powers of 100 W, 150 W, and 200 W are depicted in figure 2a. For a laser power of 100 W, only unconnected areas where a change of the surface topography occurred are visible, meaning that the melting temperature of the material was not continuously reached. A continuous line with a smoother surface than the surface of the substrate was visible in the height profile of the track produced with a laser power of 150 W. Hence, a temperature close to the melting temperature was reached continuously on the surface. A laser power of 200 W led to a broader track. It was assumed that the temperature during this process was higher than the melting temperature. Therefore, a laser power of 150 W was selected to determine the emissivity.
Multiple tracks were produced with the identified parameter combination while measuring the temperature. The laser started to emit 0.8 s before the traverse movement was activated. This initial static phase facilitated stable starting conditions during the experiments with wire feed. By changing the value of the emissivity in the software of the pyrometer, the calculated temperature could be adjusted. The measured temperatures with the independently identified $\varepsilon_1 = 0.85$, $\varepsilon_2 = 0.75$, and $\varepsilon_1/\varepsilon_2 = 1.18$ are shown in figure 2b. The diagram shows that T_{C1} and T_{C2} rose over 1600 °C as soon as the laser was activated. The temperature increased during the static phase to approximately 2200 °C. A rapid decay of the temperature was visible as soon as the laser spot was moved. During the movement phase, the mean T_{C1} and T_{C2} were 1450 °C, whereby T_{C2} was on average seven K higher than T_{C1}. In the static phase as well as in the beginning of the movement phase, T_Q deviated from T_{C1} and T_{C2} substantially and was below the melting temperature. This unexpected temperature deviation resulted from the different emissivities during the static and the movement phase caused by the different mean temperatures and surface conditions of the melt pool. The changes of ε_1 and ε_2 are indicated by the inconstant difference between T_{C1} and T_{C2}. Because T_Q strongly depends on a constant emissivity ratio, the highest differences between T_Q and T_{C1} and T_{C2} occurred during periods with a relatively high or low agreement

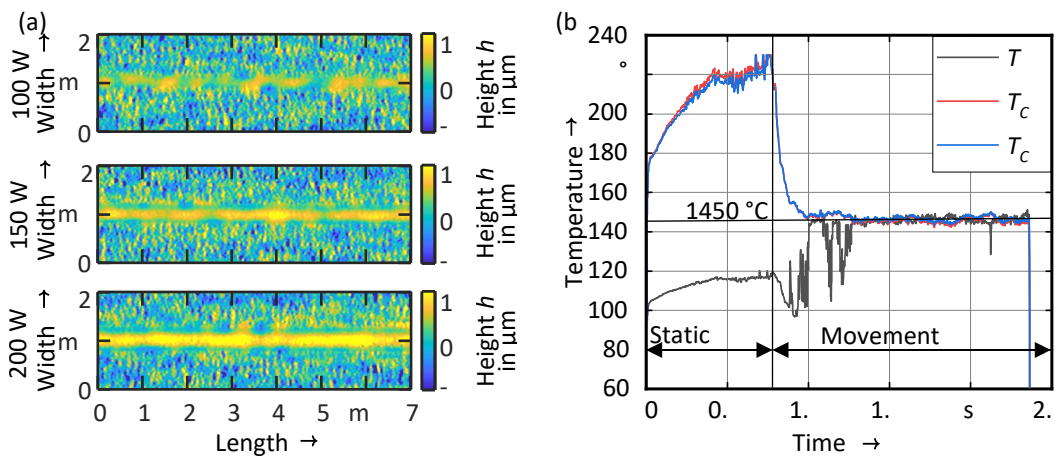

Fig. 2. (a) Height profiles for laser powers of 100 W, 150 W, and 200 W as well as (b) the temperature curves for the track with a laser power of 150 W and $\varepsilon_1 = 0.75$, $\varepsilon_2 = 0.85$, and $\varepsilon_1/\varepsilon_2 = 1.18$

between T_{C1} and T_{C2}. Only during the movement phase, where the difference between T_{C1} and T_{C2} was approximately constant, T_Q yielded reliable results. During most of the movement phase, all three temperatures approximately matched.

3.2. Temperature measurement

All temperature diagrams in figure 3 show that, during the static phase, T_{C1} and T_{C2} rose from 1600 °C to 1800 °C. During this phase, T_Q dropped from over 2000 °C to 1000 °C. This temperature drop can be explained by a substantial change of the emissivity ratio as temperatures below the melting temperature were not expected. The static phase was excluded in the analysis of the temperature signals to focus on the temperature during the movement phase.

The results of the temperature measurements with the different pyrometer spot sizes are summarized in table 2. Continuous fluctuations in the temperature of less than 50 K were categorized as “low”, fluctuations between 50 K and 300 K as “medium”, and fluctuations above 300 K as “high”.

Table 2. Summary of the temperature measurements with different setups (shown in figure 3)

Pyrometer spot size	Use of wire	Mean T_{C1} in °C	Mean T_{C2}-T_{C1} in K	Mean T_Q in °C	Fluctuation of T_{C1} and T_{C2}	Fluctuation of T_Q
Small	No	1630	7	1520	Low	High
Small	Yes	1620	7	1550	Medium	High
Medium	No	1600	15	1728	Low	Medium
Medium	Yes	1570	15	1710	Low	Medium
Large	No	1490	40	2060	Low	Medium
Large	Yes	1450	40	2110	Low	Medium

Figures 3a and 3b show the measurement results with the small pyrometer spot. For this setup, the mean tem-peratures of T_{C1}, T_{C2}, and T_Q highly match. More irregularities in the form of sudden temperature changes were measured when the wire was fed into the melt pool. This can be explained by the fact that the inner pyro-meter spot diameter was equal to the diameter of the wire. Thus, even small vibrations of the wire caused an intersection with the pyrometer spot which abruptly changed the radiance conditions. The diagrams of the temperature measurements with a medium-sized pyrometer spot in figures 3c and 3d show that, compared to the small pyrometer spot, T_{C1} and T_{C2} have a slightly higher difference in temperature of seven K. The two-color measurements showed higher mean temperatures than the one-color measurements. This can be explained by the moderately increased temperature difference between T_{C1} and T_{C2} compared to the measurements with a small pyrometer spot. The temperature measurements with a large pyrometer spot are visualized in figures 3e and 3f. These diagrams show the highest difference between T_{C1} and T_{C2} and a high increase in T_Q. The temperature difference between T_{C1} and T_{C2} was caused by changes in the wavelength-dependent emissivity within the pyrometer spot. It could be assumed that due to the temperature gradient within the melt pool, different emissivities in different areas were present. These emissivity changes differed for the two spectral ranges of measurement and thus affected the calculated temperatures. Compared with the other measurements, lower mean temperatures were measured with the large pyrometer spot. The low temperatures resulted because the large pyrometer spot covered the areas that were closer to the edge of the melt pool, where lower temperatures could be expected. The temperature fluctuations visible in the

curves in figures 3e and 3f are comparable to those present in figures 3c and 3d. These relatively small temperature fluctuations presumably resulted from the larger distance between the pyrometer spot and the wire. This distance prevented that small displacements of the wire caused an intersection with the pyrometer spot. It was assumed that most of the vibration of the wire occurred within a circle with a diameter of 1.3 mm, corresponding to the inner diameter of the middle-sized pyrometer spot.

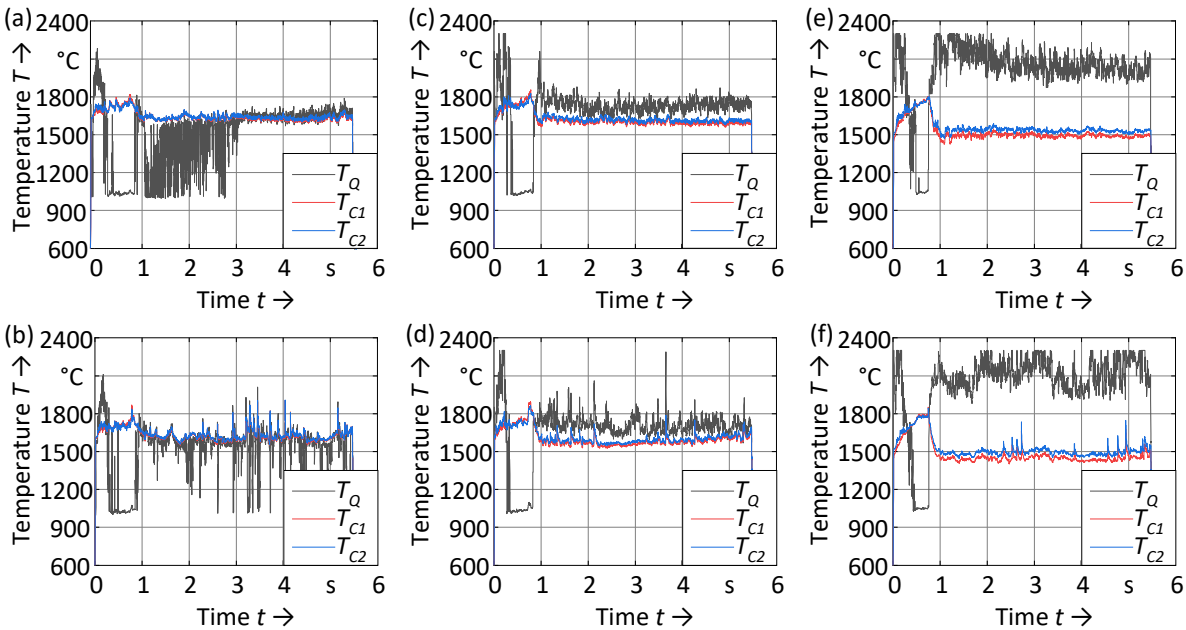

Fig. 3. Temperature curves for (a and b) a small pyrometer spot, (c and d) a medium-sized pyrometer spot, and (e and f) a large pyrometer spot; upper row: processes without wire feeding, lower row: processes with additional wire

4. Discussion

The determination of emissivities at high temperatures for the liquid phase of metals usually correlates with a high economic and temporal effort since special high-temperature devices are needed or complex simulations have to be developed (Ren et al., 2019). The proposed method, by contrast, showed a practical approach that mainly uses commercially available LMD-w setups and allows to determine the emissivity of the material of interest. However, it has to be considered that the emissivity depends on different factors such as the temperature and the properties of the surface (Altenburg et al., 2020). Therefore, the accuracy of the identified emissivity depends on the prevailing process temperature and the surface conditions of the melt pool. For process conditions closer to the calibration condition, more accurate measurements can be obtained. The best agreement of T_{C1} and T_{C2} was achieved with the small pyrometer spot, while measurements conducted with the large pyrometer spot showed the worst agreement. An increased difference between these two temperatures is an indicator for wavelength-dependent changes in the emissivity. It was assumed that the highest temperatures were continuously reached within the laser spot area and that the temperature decayed towards the border of the melt pool. Since the small pyrometer spot largely matched the laser spot (see figure 1), only minor wavelength-dependent emissivity differences resulted, which affected the temperature measurement. In contrast, the measurements with the medium-sized and large pyrometer spot covered

greater areas of the melt pool, where larger emissivity differences resulted from the temperature gradient. T_Q was affected the most in these configurations, as it strongly depended on a constant emissivity ratio. Also, the medium and high temperature fluctuations of T_Q for all measurements could be attributed to changes in the emissivity ratio, as the dynamics of the melt pool led to rapidly changing conditions on the surface of the melt pool. The results showed that the wire led to abrupt changes in the temperature signal when it intersected the small pyrometer spot. According to the measurements, these wire-induced fluctuations of the temperature could be reduced by using the middle-sized (d_i = 1.3 mm) or the large pyrometer spot (d_i = 1.6 mm).

5. Conclusion

In this work, the use of a pyrometer for the coaxial temperature measurement of a laser metal deposition process with wire was investigated. After adapting and implementing a practical method for the calibration of the pyrometer and conducting experiments while varying the size of a ring-shaped pyrometer spot, the following conclusions could be drawn:

- Identifying the emissivity of a melt pool based on the process temperature at the transition from a solid to a liquid phase led to plausible temperature values for one-color measurements.
- The wavelength-dependent changes of the emissivity of different areas of the melt pool led to large uncertainties for two-color measurements.
- Process-induced wire vibrations resulted in rapid changes in the temperature signal when the wire intersected with the pyrometer spot.
- A trade-off had to be found between lowering the influence of wire vibrations on the measurement by increasing the pyrometer spot size and lowering the influence of different emissivities within the melt pool on the measurement by reducing the pyrometer spot size.

The knowledge of the melt pool temperature is crucial to detect undesired increasing temperature changes that could lead to overheating and negatively affect the geometrical and the mechanical properties of the produced parts. Therefore, in future studies, the setup will be used to monitor the temperature during a multilayer additive process. Also, the application for temperature control will be addressed.

References

Altenburg, S., Straße, A., Gumenyuk, A., Maierhofer, C., 2020. In-situ monitoring of a laser metal deposition (LMD) process: comparison of MWIR, SWIR and high-speed NIR thermography. Quantitative InfraRed Thermography Journal, pp. 1–18.

Bi, G., Sun, C., Gasser, A., 2013. Study on influential factors for process monitoring and control in laser aided additive manufacturing. Journal of Materials Processing Technology 213 (3), pp. 463–468.

Dass, A., Moridi, A., 2019. State of the Art in Directed Energy Deposition: From Additive Manufacturing to Materials Design. Coatings 9 (7), pp. 1–26.

DebRoy, T., Wei, H., Zuback, J., Mukherjee, T., Elmer, J., Milewski, J., Beese, A., Wilson-Heid, A., De, A., Zhang, W., 2018. Additive manufacturing of metallic components – Process, structure and properties. Progress in Materials Science 92, pp. 112–224.

Everton, S., Hirsch, M., Stravroulakis, P., Leach, R., Clare, A., 2016. Review of in-situ process monitoring and in-situ metrology for metal additive manufacturing. Materials & Design 95, pp. 431–445.

Furumoto, T., Ueda, T., Alkahari, M., Hosokawa, A., 2013. Investigation of laser consolidation process for metal powder by two-color pyrometer and high-speed video camera. CIRP Annals 62 (1), pp. 223–226.

Hua, T., Jing, C., Xin, L., Fengying, Z., Weidong, H., 2008. Research on molten pool temperature in the process of laser rapid forming. Journal of Materials Processing Technology 198 (1-3), pp. 454–462.

Kelbassa, J., Biber, A., Wissenbach, K., Gasser, A., Pütsch, O., Loosen, P., Schleifenbaum, J., 2019. Influence of focal length on the laser metal deposition process with coaxial wire feeding. Proceedings of SPIE 10911, #109110D.

Kuznetsov, A., Jeromen, A., Levy, G., Fujishima, M., Govekar, E., 2016. Annular Laser Beam Cladding Process Feasibility Study. Physics Procedia 83, pp. 647–656.

Liu, S., Kong, F., Shi, S., Kovacevic, R., 2014. Study of a hollow laser beam for cladding. Journal of Advanced Manufacturing Technology 73 (1-4), pp. 147–159.

Mates, S., Basak, D., Biancaniello, F., Ridder, S., Geist, J., 2002. Calibration of a Two-Color Imaging Pyrometer and its Use for Particle Measurements in Controlled Air Plasma Spray Experiments. Journal of Thermal Spray Technology 11, pp. 195–205.

Mohr, P., Taylor, B., Newell, D., 2012. CODATA recommended values of the fundamental physical constants: 2010. Reviews of Modern Physics 84, p. 1591.

Müller, B., Renz, U., 2001. Development of a fast fiber-optic two-color pyrometer for the temperature measurement of surfaces with varying emissivities. Review of Scientific Instruments 72 (8), pp. 3366–3374.

Nair, A., Muvvala, G., Sarkar, S., Nath, A., 2020. Real-time detection of cooling rate using pyrometers in tandem in laser material processing and directed energy deposition. Materials Letters 277, #128330.

Ren, C., Lo, Y., Tran, H., Lee, M., 2019. Emissivity calibration method for pyrometer measurement of melting pool temperature in selective laser melting of stainless steel 316L. Journal of Advanced Manufacturing Technology 105 (1-4), pp. 637–649.